Experimental and Molecular Pathology 129 (2022) 104848

Contents lists available at ScienceDirect

Experimental and Molecular Pathology

journal homepage: www.elsevier.com/locate/yexmp

Expression analysis of hsa_circ_0020397, hsa_circ_0005986, hsa_circ_0003028, and hsa_circ_0006990 in renal cell carcinoma

Elham Mohammadisoleimani [a,b], Zahra Firoozi [c], Mohammad Mehdi Naghizadeh [d], Ali Ghanbari Asad [a], Anahita Jafari [e], Mohammad Hosein Pourjafarian [b], Ali Ariafar [e], Hosein Mansoori [d], Hassan Dastsooz [f,g,h], Hani Sabaie [i], Shahryar Zeighami [j,**], Yaser Mansoori [c,d,*]

[a] Department of Medical Biotechnology, Fasa University of Medical Sciences, Fasa, Iran
[b] USERN Office, Fasa University of Medical Sciences, Fasa, Iran
[c] Department of Medical Genetics, Fasa University of Medical Sciences, Fasa, Iran
[d] Noncommunicable Diseases Research Center, Fasa University of Medical Sciences, Fasa, Iran
[e] Urology Oncology Research Center, Shiraz University of medical sciences, Shiraz, Iran
[f] IIGM-Italian Institute for Genomic Medicine, c/o IRCCS, Candiolo, Torino, Italy
[g] Candiolo Cancer Institute, FPO-IRCCS, Candiolo Cancer (IT), Torino, Italy
[h] Department of Life Sciences and Systems Biology, University of Turin, Via Accademia Albertina, 13, Turin 10123, Italy
[i] Department of Medical Genetics, Faculty of Medicine, Tabriz University of Medical Sciences, Tabriz, Iran
[j] Urology Department, Shiraz University of Medical Sciences, Shiraz, Iran

ARTICLE INFO

Keywords:
Renal cell carcinoma
ceRNA
hsa_circ_0020397
hsa_circ_0005986
hsa_circ_0003028
hsa_circ_0006990

ABSTRACT

Renal cell carcinoma (RCC) is a prevalent heterogeneous kidney cancer. So far, different genes have been reported for RCC development. However, its particular molecular mechanism remains unclear. Circular RNAs (circRNAs), a class of non-coding RNAs, are involved in numerous biological processes in different malignancies such as RCC. This study aims to assess the expression and underlying mechanism of four circRNAs (hsa_circ_0020397, hsa_circ_0005986, hsa_circ_0003028, hsa_circ_0006990) with possible new roles in RCC. In the experimental step, we investigated the expression of these four circRNAs in our RCC samples using quantitative real-time polymerase chain reaction. In the bioinformatics step, the differential expressed mRNAs (DEmRNAs), and miRNAs (DEmiRNAs) were obtained from the GEO datasets using the GEO2R tool. A protein-protein interaction network was constructed using the STRING database, and hub genes were identified by Cytoscape. Molecular pathways associated with hub genes were detected using KEGG pathway enrichment analysis. Then, we utilized the ToppGene database to detect the relationships between DEmiRNAs and hub genes. Furthermore, interactions between circRNAs and DEmiRNAs were predicted by the StarBase and circinteractome databases. Finally, a circRNA-DEmiRNA-hub gene triple network was constructed. Our results revealed that the expression of hsa_circ_0020397, hsa_circ_0005986, and hsa_circ_0006990 was downregulated in RCC tissues. Moreover, these circRNAs had a significantly lower expression in patients with a history of kidney disease. Furthermore, hsa_circ_0003028 and hsa_circ_0006990 showed higher expression in the tumor of participants with Lymphovascular/perineural invasion and oncocytoma type, respectively. Based on bioinformatic results, 15 circRNA-DEmiRNA-hub gene ceRNA regulatory axes were predicted, which included three hub genes, five miRNAs, and four selected circRNAs. In conclusion, the current work is the first to emphasize the expression of the

Abbreviations: CASP8, Caspase 8; CCND1, Cyclin D1; ccRCC, Clear cell renal cell carcinoma; ceRNA, Competing endogenous RNA; circRNA, Circular RNA; CRC, Colorectal cancer; CYCS, Cytochrome C; DEG, Differential expressed genes; DEmiRNA, Differential expressed miRNA; DEmRNA, Differential expressed mRNA; GEO, Gene expression omnibus; HCC, Hepatocellular carcinoma; KEGG, Kyoto Encyclopedia of Genes and Genomes; PPI, Protein-protein interaction; qPCR, Quantitative polymerase chain reaction; miRNA, microRNA; ncRNA, non-coding RNA; RCC, Renal cell carcinoma.

* Correspondence to: Yaser mansoori, Noncommunicable Diseases Research Center, Fasa University of Medical Sciences, Fasa, Iran.
** Correspondence to: Shahryar Zeighami, Urology Department, Shiraz University of Medical Sciences, Shiraz, Iran.
E-mail address: y.mansouri@fums.ac.ir (Y. Mansoori).

https://doi.org/10.1016/j.yexmp.2022.104848
Received 29 August 2022; Received in revised form 29 November 2022; Accepted 5 December 2022
Available online 7 December 2022

hsa_circ_0020397, hsa_circ_0005986, hsa_circ_0003028, and hsa_circ_0006990 in RCC patients presents a novel perspective on the molecular processes underlying the pathogenic mechanisms of RCC.

1. Introduction

Renal cell carcinoma (RCC) is the most frequent kidney malignancy and accounts for approximately 90–95% of all types of kidney cancers. RCC is categorized into different specific subtypes, including clear cell, papillary, chromophobe, cystic-solid, collecting ducts, medullary, and other rare subtypes. The three first subtypes are accounted for >90% of RCCs (Muglia and Prando, 2015). Clear cell RCC (ccRCC) is the most common subtype with a less favorable prognosis than other subtypes. Surgical excision is the cornerstone treatment for localized ccRCC. However, 30% of patients with localized ccRCC eventually experience recurrence and metastasis, leading to a significant case-fatality rate (Hsieh et al., 2017; De Meerleer et al., 2014). Nearly 60% of stage IV patients die within 2–3 years after diagnosis (Mendoza-Alvarez et al., 2019). The prognosis is dismal despite significant advancements in diagnosis and the 5-year survival rate (Moch et al., 2014; Chen et al., 2020). In order to effectively treat RCC, especially ccRCC, it is critical to thoroughly assess the molecular underpinnings of pathogenesis, uncover new prognostic biomarkers, and develop therapeutic targets. Various genetic and epigenetic factors can influence the development and treatment response of RCC patients (Arai and Kanai, 2010). In the past ten years, a family of non-coding RNAs (ncRNAs), which includes microRNAs (miRNAs), long non-coding RNAs (lncRNAs), and circular RNAs (circRNAs), have been discovered to be potent regulators of several genes and pathways implicated in the onset and progression of malignancies, including RCC (Toraih et al., 2022). Non-coding RNAs (ncRNAs) account for the vast majority of RNA molecules, but for a long time they were considered transcriptional junk. In recent years, increased transcriptome sequencing led to the identification of circular RNAs, a new type of non-coding RNA (Santer et al., 2019).

CircRNAs are various and widespread in mammals. They are stable and closed-loop structures, with the majority of them not being degraded by RNA exonuclease or RNAase. (Li et al., 2018). CircRNAs naturally play a part in numerous biological processes, including replication, transcriptional control, RNA processing intermediates, and translation mediation, all of which are essential for the development of numerous organs and the maintenance of cell pluripotency (Zhang et al., 2018; Sayad et al., 2022). Moreover, as a new regulatory mechanism, the competing endogenous RNA (ceRNA) hypothesis states that circRNAs might operate as miRNA "sponges" by competing with target mRNAs for binding to miRNAs (Abdollahzadeh et al., 2019; Salmena et al., 2011). MiRNAs, a class of ncRNAs with an average of 22 nucleotides, have played critical roles in various biological processes and normal development, such as RNA silencing (O'Brien et al., 2018) and Resistance to cancer chemotherapy drugs is one of the main barriers to the formation and development of cancer (Si et al., 2019). MiRNA can influence gene expression at the post-transcriptional stage by degrading the target mRNA or inhibiting its translation (Ankasha et al., 2018). CircRNAs bind to miRNA to regulate their function. The interaction of miRNA with different regions of target mRNAs is dynamic and dependent on various factors; thus, circRNA regulates the expression of mRNAs indirectly (Bai et al., 2020). So far, most studies in the field of ceRNA mechanism have been focused on cancers (Ala, 2020). In the latest RCC research, studies have demonstrated that the ceRNA network played a key role in the development of RCC (Bai et al., 2020; Jiang and Ye, 2019). We aimed to examine the role of four circRNAs, namely; hsa_circ_0020397, hsa_circ_0005986, hsa_circ_0003028, and hsa_circ_0006990 in RCC pathogenesis. Hsa_circ_0020397 circRNA is originated from the dedicator of cytokinesis 1 (*DOCK1*), and it may play a part in the development and spread of breast and colorectal cancer (CRC) (Glažar et al., 2014; Kurosaki et al., 2021; Zhang et al., 2017). Zhang et al. investigated the role of *DOCK1* in RCC. The results of this

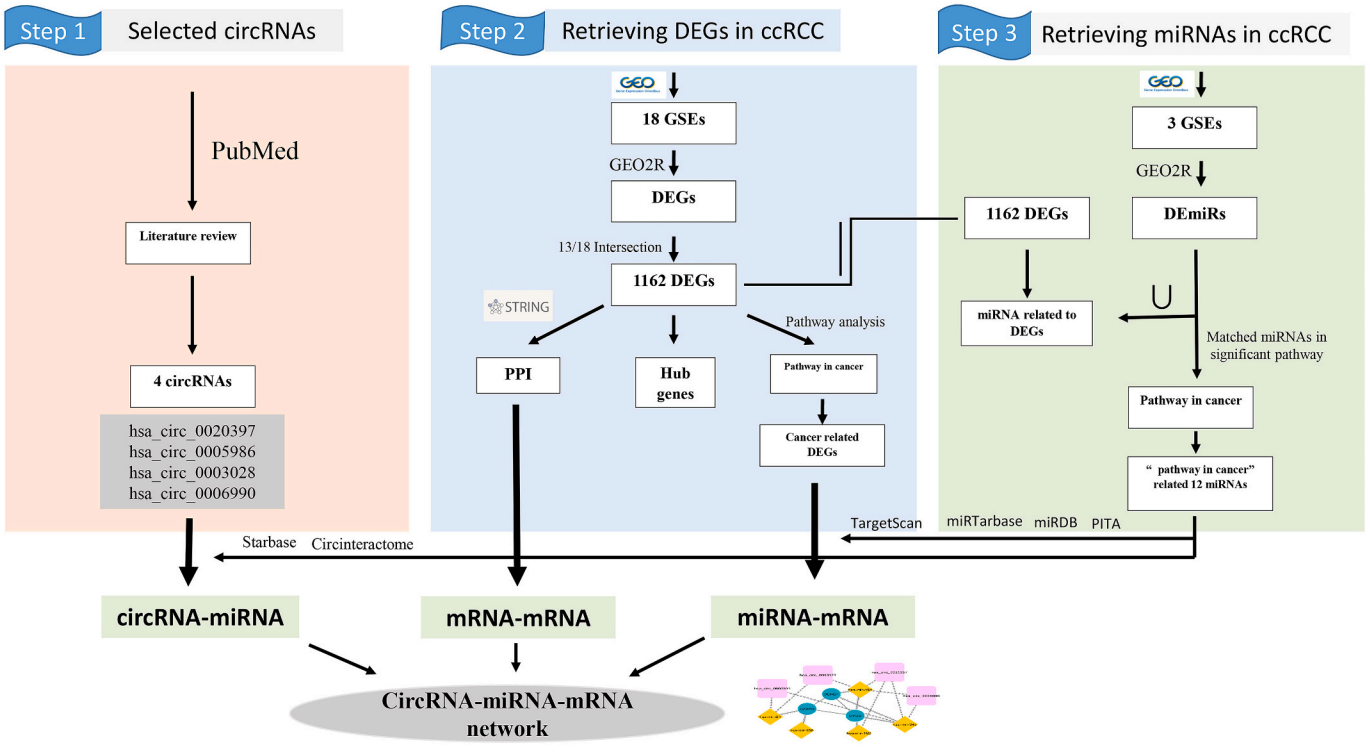

Fig. 1. The overall workflow of our bioinformatics analyses.

Table 1
QRT-PCR primer sequences.

Genes	Forward (5′–3′)	Reverse (5′–3′)
β2M	AGATGAGTATGCCTGCCGTG	GCGGCATCTTCAAACCTCCA
hsa_circ_0005686	CTATAAAACTTTAAAGAACACTACTGAGCC	GGGTCTTGTCAACAGCAGAA
hsa_circ_0020397	GAGATTCTGAACTCATTCTTTTTATAACT	GCAGGAAATATACCCTTCTTAGAC
hsa_circ_0003028	GAATCTCTCCGCATGTAGAGC	CAGGTGAATAGACTTCTGTTGTTTC
hsa_circ_0006990	GATAAATTGGCCCCTTCACAGA	CCCTGGGTCAATAATTCCACTG

Abbreviation: β2M, Beta-2-Microglobulin; qRT-PCR, Quantitative Reverse Transcription Polymerase Chain Reaction.

study indicate that *DOCK1* is crucial for RCC cells' chemoresistance to cisplatin (Zhang et al., 2020). Hsa_circ_0005986, which is originated from PR/SET domain 2 (*PRDM2*) (Glažar et al., 2014), has a potential relevance as a predictive biomarker in hepatocellular carcinoma (HCC) patients. The expression of *PRDM2* is associated with copy number alteration (CNA), and it is significant in the comparison of mRNA expression between ccRCC and non-ccRCC kidney cancer subtypes (Yan et al., 2019). Hsa_circ_0003028, derived from the fucosyltransferase 8 (*FUT8*) gene (Glažar et al., 2014), was introduced as a biomarker in non-small cell lung cancer (Li et al., 2021). Hsa_circ_0006990, located on chr18, is derived from the VAMP-associated protein A (*VAPA*) gene (Glažar et al., 2014). This circRNA is a promising biomarker for CRC (Li et al., 2019). The VAPA can function as a miRNA sponge for PTEN (Mendoza-Alvarez et al., 2019). PTEN is a candidate tumor suppressor gene in renal cell carcinoma (RCC). This gene regulates cell cycle progression and cell survival in this cancer (Shin Lee et al., 2003). To our knowledge, the expression pattern and functions of these four circRNAs in RCC remain a mystery. CircRNAs have emerged as potential biomarkers for the prognosis and diagnosis of RCC as well as targets for the development of new treatments. However, additional research is required to comprehend the roles of circRNAs in RCC (Wang et al., 2020).

The overall aim of the current study is to evaluate the expression of four circRNAs (i.e., hsa_circ_0020397, hsa_circ_0005986, hsa_circ_0003028, and hsa_circ_0006990) in RCC and construct their corresponding ceRNA networks using experimental and bioinformatics approaches, respectively.

2. Materials and methods

2.1. The workflow of the study

Using the PubMed database, we searched for a selection of recently identified circRNAs confirmed by previous studies. So four circRNAs (hsa_circ_0020397, hsa_circ_0005986, hsa_circ_0003028, and hsa_circ_0006990) were selected. By looking up information in the Pubmed database (https://pubmed.ncbi.nlm.nih.gov/), we discovered that recent research has focused on the regulating effects of four circRNAs in cancer development but its role in regulating other diseases, such as RCC, had not been explored. Additionally, studies show these circRNAs can regulate their parental genes (Li et al., 2015). Parental genes related to selection's circRNAs play a role in the pathogenesis of RCC. Then, we evaluated their expression in RCC using quantitative polymerase chain reaction (qPCR). In the following, we used bioinformatics approaches to find out their potential mechanism in the progression of RCC based on ceRNA theory. Therefore, we constructed the ceRNA network related to the selected circRNAs using circRNA-DEmiRNA (differential expressed miRNAs) and DEmiRNA-hub genes interactions. A summary of the bioinformatics analyses workflow is shown in Fig. 1. More details of each step are provided in the following sub-sections.

2.2. QPCR analysis

2.2.1. Patient characteristics and tissue collection

To perform the present case-control study, forty samples of RCC tissues and their adjacent normal tissues were obtained from patients at the Ali-Asghar, Namazi, and Ghadir Mother and Child Hospitals, Shiraz, Iran. In these hospitals, a pathologist gave the final diagnosis of renal cell carcinoma and its different types. Also, patients were divided into four subtypes that included 27 (67.5%) clear cells, 5 (12.5%) papillaries, 6 (15%) chromophobes, and 2 (5%) oncocytomas (Supplementary File 1). All RCC specimens were immediately snap-frozen in liquid nitrogen and stored at −80 °C for later use. Ethical approval of this study was granted by the Fasa University of Medical Sciences research ethics committee (ethical code: IR.FUMS.REC.1398.147).

2.2.2. RNA isolation, complementary DNA (cDNA) synthesis, and qPCR

Total cellular RNA was prepared using TRIzol isolation reagent (Invitrogen, Thermo Fisher) following the manufacturer's recommendations. Due to the higher density of the cells, the amount of tissue used for tumor samples is between 50 and 100 mg and 200 mg for normal samples, and both types of tissue are homogenized with 1000 μl of TRIzol. To assess RNA quality and quantity, first run intact total RNA through a 1% agarose gel electrophoresis, which reveals distinct 28S and 18S rRNA bands. The band of the 28S rRNA should be around double that of the 18S rRNA band. Secondly, the A260/A280 ratio of pure RNA is in the range of $\geq$1.6 and $>$ 2.0. Lastly, we repeated the RNA extraction process on a set of samples. The amount of RNA was normalized in each sample. We utilized the DNase I treatment to remove genomic DNA, and there were no bands ($>$10 kb) or smears on the agarose gel after the RNA samples were run through it. Then, cDNA synthesis was done using the PrimeScript™ RT Reagent Kit (Takara, Cat.No: RR037A), following the manufacturer's recommendations. The amount of cDNA is about 4000 ng for each sample. Next, qPCR was carried out by Power SYBR® Green PCR Master Mix (ABI, USA) on the 7500 real-time PCR system (ABI, life technology). Thermal cycling conditions are: polymerase activation at 95 °C for 15 min, replication at 94 °C for 30 s, and then 60 °C for 30 s by 45 cycles, with a melt curve at 60–95 °C for 60 min. The expression level of beta-2 microglobulin (*β2M*) was used as an internal control for quantitative PCR. In each run, B2M was placed along with the samples, and we measured the data of each run against the B2M expression in the same run. Melt curve analysis and gel electrophoresis are used on PCR products to look for primer dimers or non-specific amplification. Primer sequences for hsa_circ_0020397, hsa_circ_0005986, hsa_circ_0003028, hsa_circ_0006990, and *β2M* are shown in Table 1. At the back-splice junction of circRNAs, divergent primers were designed, referring to previous studies (Panda and Gorospe, 2018; Zhong et al., 2018a). The standard curve is used to ensure specificity and efficiency. All reactions were done in triplicate. The relative expression levels of circRNAs and B2M were determined using $2^{-\Delta\Delta Ct}$, and CTs for each circRNA were normalized against B2M. The REST 2009 software was used for data analysis of qPCR.

2.2.3. Statistical analysis

Data analyses were carried out in IBM SPSS 21 software (IBM SPSS Corp, Armonk, NY), and the level of *P*-value $<$0.05 was regarded as significant. The comparison of fold change between tumors and their adjacent non-cancerous tissues was performed by the Wilcoxon test. Mann-Whitney and Kruskal-Wallis tests were used to assess the relation between circRNAs expression with demographic and clinicopathological

Table 2
Essential characteristics of the eighteen GEO datasets.

Data source	Platform	Number of samples	Number of controls	Number of tumors	number of degS
GSE781	GPL96	34	8	9	3040
GSE781	GPL97	34	8	9	785
GSE6344	GPL96	40	10	10	5533
GSE6344	GPL97	40	10	10	3396
GSE14994	GPL3921	229	11	59	8024
GSE16441	GPL6480	68	17	17	10,470
GSE17816	GPL9101	45	9	36	1694
GSE17818	GPL9101	115	13	102	9035
GSE17895	GPL9101	160	22	138	7373
GSE26574	GPL11433	67	8	8	4623
GSE36895	GPL570	76	23	28	11,251
GSE40435	GPL10558	202	101	101	13,468
GSE40914	GPL3985	80	22	58	738
GSE46699	GPL570	130	56	74	14,202
GSE53000	GPL6244	62	6	53	5330
GSE53757	GPL570	144	34	86	14,614
GSE68417	GPL6244	49	14	29	8803
GSE71963	GPL6480	48	16	32	8106

Table 3
Essential characteristics of the three miRNA expression profiles datasets used in ccRCC.

Data source	Platform	Number of samples	NUMBER OF CONTROLS	NUMBER OF TUMORS	NUMBER OF DEmirNAs
GSE16441	GPL8659	34	17	17	123
GSE55138	GPL14613	25	9	16	94
GSE41282	GPL8786	38	5	6	49

features of RCC patients. According to the median fold changes for each gene, samples were divided into two groups of high and low expressions, and the differences among these groups were achieved by chi-square test and independent *t*-test.

2.3. Bioinformatics analysis

2.3.1. Identification of differential expression mRNAs (DEmRNAs) in ccRCC

We searched gene expression omnibus (GEO) database to identify array expression profiling studies (GSE781, GSE781, GSE6344, GSE6344, GSE14994, GSE16441, GSE17816, GSE17818, GSE17895, GSE26574, GSE36895, GSE40435, GSE40914, GSE46699, GSE53000, GSE53757, GSE68417, GSE71963) (Table 2, Supplementary Files 2) (Edgar et al., 2002). Studies containing gene expression profiles of normal and ccRCC tissues and compatibility with the GEO2R were considered. After analyzing the data with the GEO2R, in per GSE, the genes with a false discovery rate (adjusted *P*-value) < 0.05 were selected. Common shared DEmRNAs that were present in >13 GSEs were selected for further analysis.

2.3.2. Identification of differentially expressed miRNAs

The GEO database was applied to search for "microRNA" AND "renal cell carcinoma" keywords to identify miRNA microarray studies. We selected studies whose experiment type was specified as "non-coding RNA profiling by array" (Table 3). First, we performed the GEO2R analysis, and the miRNAs with adjusted *P*-value <0.05 was identified as DEmiRNAs.

2.3.3. Establishment of protein-protein interaction (PPI) network and identification of hub genes

The STRING database (https://string-db.org/) helps to merge functional associations and physical interactions between proteins (Szklarczyk et al., 2019). DEmRNAs identified in >13 GSEs were selected as the input to the STRING database. PPIs were mapped with this database and visualized with Cytoscape software (version 3.7.2) (Shannon et al., 2003). The Hub genes were identified using centrality measurements (Degree, Betweenness, Closeness and Eigenvector) by Cytoscape. Overlapping, top-ranking genes among the four calculation methods were chosen as hub genes.

2.3.4. Investigation of DEmiRNA-DEmRNA, circRNA-DEmiRNA interactions, and construction of ceRNA network

In this step, we distinguished miRNAs related to the DEmRNAs, as well as miRNAs targeting DEmRNAs in "Pathways in cancer" using the ToppGene database. The miRTarbase (http://miRTarBase.mbc.nctu.edu.tw/), miRDB (http://mirdb.org/), PITA (https://www.ebi.ac.uk/thornton-srv/databases/pita/), and Targetscan (http://www.targetscan.org/vert_72/) were considered as selected databases for the ToppGene query. On the other hand, the interactions of hsa_circ_0020397, hsa_circ_0005986, hsa_circ_0003028, and hsa_circ_0006990 with DEmiRNAs were explored. CircRNA-DEmiRNA interactions were predicted using the starbase database (http://starbase.sysu.edu.cn/) and Circular RNA Interactome (https://circinteractome.nia.nih.gov/). We checked the context score percentile above 75 in circintractome to ensure the correctness of forecast results. Finally, the circRNA-DEmiRNA-hub genes triple network was constructed and visualized with Cytoscape software.

2.3.5. Kyoto encyclopedia of genes and genomes (KEGG) pathway enrichment analysis

At this stage, utilizing the ToppGene database, we carried out a KEGG pathway enrichment study to carry out the analysis on significant pathways involving all DEGs. For KEGG pathways, the false discovery rate (FDR) cutoff of <0.05 was determined. The most common genes and the most genes annotated were the criteria for pathway selection.

2.3.6. Survival analysis

We used the Gene Expression Profiling Interactive Analysis (GEPIA) database to evaluate the association between hub genes in the ceRNA network and the survival of RCC patients based on the Log-rank test using The Cancer Genome Atlas (TCGA) data (Tang et al., 2017).

3. Results

3.1. QPCR results

3.1.1. The expression of hsa_circ_0020397, hsa_circ_0005986, hsa_circ_0003028 and hsa_circ_0006990 in tumors and adjacent normal tissues

The evaluation of circRNAs expression in our 40 RCC tumor samples and their adjacent non-cancerous tissues revealed that the expression of hsa_circ_0020397, hsa_circ_0005986 and hsa_circ_0006990 were significantly lower in tumors (Tumor Median = 0.095, 0.162, 0.670, respectively) than their adjacent normal tissues (Normal Median = 1.056, 0.932, 0.948, respectively) (*P*-value = 0.004, 0.000062, 0.042, respectively). However, the expression of hsa_circ_0003028 did not differ between tumor and adjacent tissue samples (*P*-value = 1.000) (Fig. 2, Table 4).

The analysis of circRNAs expressions in 27 ccRCC samples revealed relatively lower expressions of hsa_circ_0020397, hsa_circ_0005986 and hsa_circ_0006990; while hsa_circ_0003028 was similarly expressed in ccRCC and adjacent tissue samples (Table 5). Also, the comparison of circRNAs expression between tumors and adjacent non-cancerous tissues in non-ccRCC revealed relatively lower expression of hsa_circ_0005986 (Table 6).

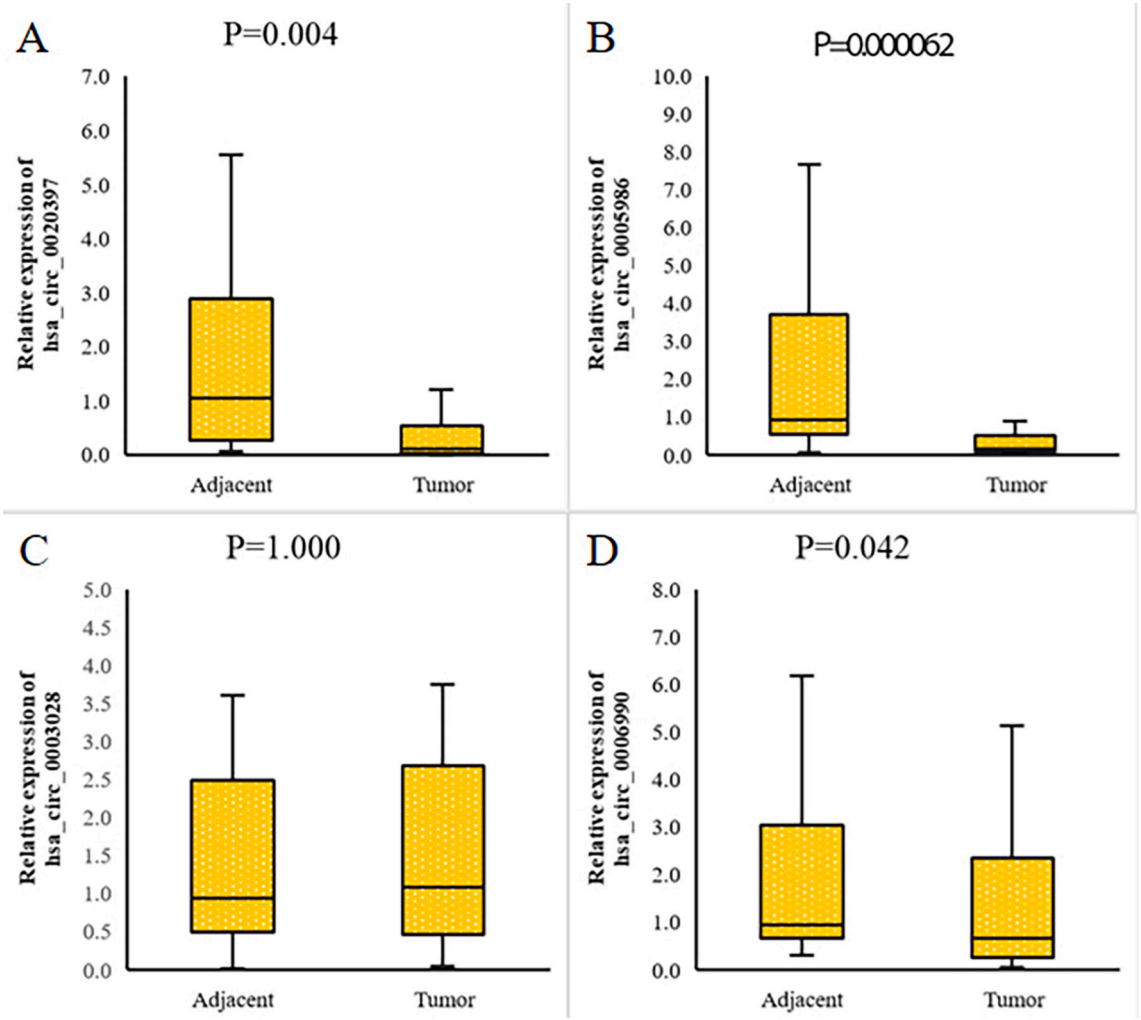

Fig. 2. The box plot for comparing the expression of (A) hsa_circ_0020397, (B) hsa_circ_0005986, (C) hsa_circ_0003028, and (D) hsa_circ_0006990 between tumors and adjacent non-cancerous tissues.

Table 4
The comparison of circRNAs expression between tumors and adjacent non-cancerous tissues in all types of RCC. All *P*-values were computed from the Wilcoxon test.

	Valid N	Mean	Standard Deviation	Median	*P*-value
FC_N_0020397	40	17.059	73.195	1.056	0.004
FC_T_0020397	40	1.241	3.860	0.095	
FC_N_0005986	40	18.549	47.924	0.932	0.000062
FC_T_0005986	40	0.599	1.477	0.162	
FC_N_0003028	40	5.544	19.947	0.935	1.000
FC_T_0003028	40	3.565	10.415	1.091	
FC_N_0006990	40	1.988	2.455	0.948	0.042
FC_T_0006990	40	1.493	1.880	0.670	

3.1.2. The association of hsa_circ_0020397, hsa_circ_0005986, hsa_circ_0003028 and hsa_circ_0006990 expression with demographic and clinicopathological characteristics of RCC patients

Our data revealed that hsa_circ_0020397, hsa_circ_0005986 and hsa_circ_0006990 had a significant lower expression in patients who had history of kidney disease (*P*-value = 0.026, 0.008, 0.028, respectively) (Fig. 3a, b, c, Table 7). In addition, hsa_circ_0003028 had a higher expression in the tumor of participants with Lymphovascular/perineural invasion (*P*-value = 0.022, Fig. 3d), and hsa_circ_0006990 had a higher expression in oncocytoma type in comparison to other types of RCC (*P*-

Table 5
The comparison of circRNAs expression between tumors and adjacent non-cancerous tissues in ccRCC. All p-values computed from the Wilcoxon test.

	Valid N	Mean	Standard Deviation	Median	*P*-value
FC_N_0020397	27	24.304	88.673	1.060	0.005
FC_T_0020397	27	1.036	3.926	0.028	
FC_N_0005986	27	23.878	56.965	0.772	0.002
FC_T_0005986	27	0.681	1.782	0.133	
FC_N_0003028	27	7.139	24.130	0.993	0.981
FC_T_0003028	27	4.606	12.598	1.110	
FC_N_0006990	27	2.009	2.757	0.918	0.002
FC_T_0006990	27	0.933	1.187	0.425	

Table 6
The comparison of circRNAs expression between tumors and adjacent non-cancerous tissues in non-ccRCC. All p-values computed from the Wilcoxon test.

	Valid N	Mean	Standard Deviation	Median	*P*-value
FC_N_0020397	13	2.012	3.502	0.910	0.279
FC_T_0020397	13	1.666	3.840	0.377	
FC_N_0005986	13	7.481	15.389	1.245	0.013
FC_T_0005986	13	0.429	0.404	0.208	
FC_N_0003028	13	2.231	3.735	0.693	0.917
FC_T_0003028	13	1.402	1.061	1.000	
FC_N_0006990	13	1.944	1.765	0.977	0.552
FC_T_0006990	13	2.656	2.501	2.390	

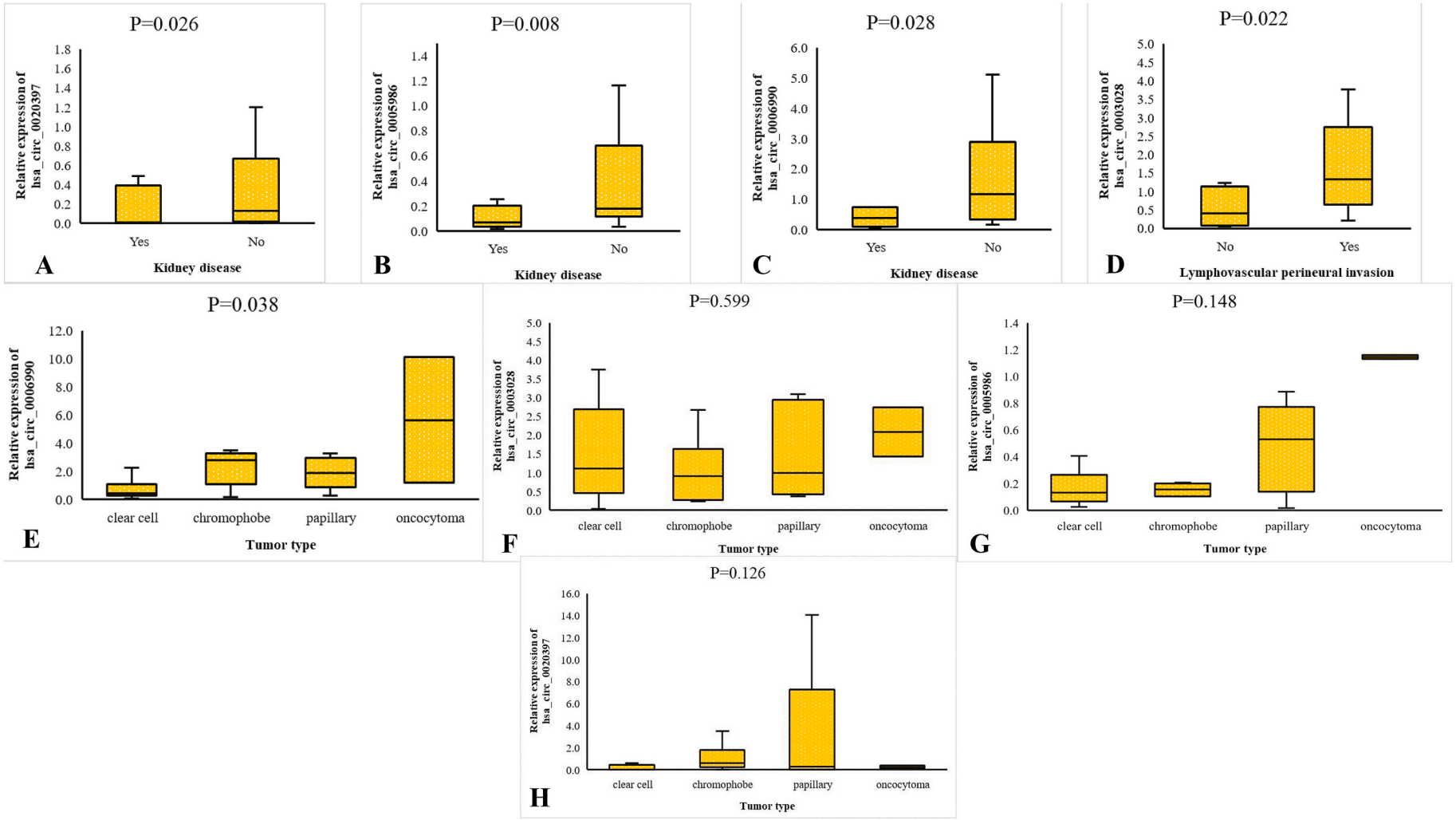

Fig. 3. The box plot for comparing the expression of (A) hsa_circ_0020397, (B) hsa_circ_0005986, and (C) hsa_circ_0006990 in patients with or without kidney disease. (D) The box plot to compare the expression of hsa_circ_0003028 in patients with or without lymphovascular/perineural invasion. (E) The box plot for the expression comparison of hsa_circ_0006990 in different subtypes of RCC. The comparison of expression in different types of RCC in hsa_circ_0003028 (F), hsa_circ_0005986 (G), and hsa_circ_0020397 (H). The comparison of expression in different types of RCC was measured two by two by the Mann-Whitney test. The following are significant *P*-values: The P-value for chromophore and oncocytoma is 0.046; the P-value for clear cell and chromophore is 0.025; and the P-value for clear cell and chromophore is 0.032.

Table 7
The Association of hsa_circ_0020397, hsa_circ_0005986, hsa_circ_0003028, and hsa_circ_0006990 expression with demographic and clinicopathological features in RCC patients.

Table 7		hsa_circ_0020397					hsa_circ_0005986				hsa_circ_0003028				hsa_circ_0006990			
		N	Mean	SD	Median	*P*-value	Mean	SD	Median	*P*-value	Mean	SD	Median	*P*-value	Mean	SD	Median	*P*-value
Sex	Male	29	1.562	4.498	0.077	0.809	0.742	1.717	0.178	0.820	3.409	11.292	1.000	0.332	1.466	1.990	0.731	0.458
	Female	11	0.393	0.605	0.125		0.221	0.191	0.135		3.975	8.109	1.705		1.566	1.640	0.524	
Tumor size	≤4	20	0.183	0.230	0.065	0.152	0.719	1.935	0.205	0.344	4.355	13.566	1.091	0.766	1.430	2.288	0.441	0.417
	>4	20	2.299	5.308	0.280		0.479	0.841	0.124		2.774	6.107	1.111		1.556	1.417	1.258	
Tumor focality	focal	25	0.810	2.807	0.032	0.230	0.789	1.822	0.208	0.364	4.859	13.068	1.072	0.625	1.509	2.086	0.731	0.856
	unifocal	15	1.960	5.207	0.280		0.282	0.464	0.133		1.408	1.202	1.110		1.467	1.544	0.434	
Tumor type	Clear cell	27	1.036	3.926	0.028	0.126	0.681	1.782	0.133	0.148	4.606	12.598	1.110	0.599	0.933	1.187	0.425	**0.038**
	Papillary	5	2.977	6.201	0.280		0.471	0.340	0.531		1.547	1.309	1.000		1.905	1.158	1.849	
	Chromophore	6	1.047	1.274	0.626		0.155	0.046	0.156		1.050	0.893	0.905		2.290	1.294	2.761	
	Oncocytoma	2	0.246	0.186	0.246		1.146	0.022	1.146		2.093	0.931	2.093		5.634	6.323	5.634	
Tumor necrosis	Seen	20	2.054	5.359	0.073	0.745	0.729	1.968	0.123	0.068	4.112	13.620	0.905	0.079	1.622	2.314	0.821	0.626
	Not seen	20	0.428	0.691	0.101		0.469	0.756	0.200		3.017	6.042	1.570		1.365	1.365	0.567	
Fuhrman nuclear grade	1	5	0.807	1.517	0.125	0.992	0.441	0.463	0.178	0.938	1.535	1.171	1.292	0.281	2.670	4.256	0.425	0.989
	2	21	0.352	0.575	0.077		0.371	0.735	0.160		4.252	13.234	1.000		1.189	1.111	0.610	
	3	9	0.407	0.660	0.028		1.241	2.875	0.178		4.580	8.941	1.434		1.349	1.606	0.912	
	4	5	6.910	9.712	0.034		0.559	0.769	0.131		0.880	1.280	0.344		1.854	1.606	2.670	
Lymph vascular perineural invasion	No	8	4.324	8.163	0.019	0.223	0.359	0.643	0.072	0.073	0.770	1.028	0.410	**0.022**	1.278	1.454	0.397	0.543
	Yes	32	0.470	0.795	0.120		0.659	1.623	0.178		4.264	11.563	1.334		1.547	1.988	0.821	
Extension	No	30	0.408	0.770	0.095	0.815	0.650	1.679	0.170	0.803	3.551	11.061	1.257	0.190	1.379	1.950	0.533	0.532
	Yes	10	3.740	7.307	0.157		0.445	0.581	0.124		3.608	8.707	0.660		1.837	1.700	1.681	
Cancer history	No	19	0.437	0.711	0.054	0.735	0.859	2.095	0.133	0.481	1.433	1.167	1.110	0.871	1.929	2.433	1.077	0.350
	Yes	21	1.968	5.237	0.113		0.364	0.429	0.203		5.494	14.215	1.000		1.099	1.104	0.456	
BMI	≤25	9	4.340	7.577	0.388	0.221	0.414	0.568	0.203	0.578	1.527	1.001	1.000	0.408	1.734	1.338	1.837	0.309
	25–29	26	0.368	0.631	0.043		0.708	1.798	0.144		3.627	11.929	1.036		1.166	1.294	0.578	
	≥30	5	0.200	0.232	0.115		0.365	0.449	0.116		6.911	11.953	1.705		2.763	4.191	0.524	
Kidney disease	No	29	1.660	4.481	0.125	**0.026**	0.771	1.707	0.178	**0.008**	2.435	5.084	1.292	0.310	1.823	2.084	1.162	**0.028**
	Yes	11	0.136	0.201	0.009		0.145	0.196	0.068		6.543	18.363	0.993		0.624	0.692	0.368	

P-values less than 0.05 were considered to be statistically significant.

Table 8
The Association of hsa_circ_0020397, hsa_circ_0005986, hsa_circ_0003028, and hsa_circ_0006990 expression with demographic and clinicopathological features in RCC patients, according to dividing fold changes into two groups of high and low expressions.

Table 8		hsa_circ_0020397				*P*-value	hsa_circ_0005986				*P*-value	hsa_circ_0003028				P-value	hsa_circ_0006990				*P*-value
		Low		High			Low		High			Low		High			Low		High		
		N	%	N	%		N	%	N	%		N	%	N	%		N	%	N	%	
Tumor size	≤4	11	55.0%	9	45.0%	0.527	8	40.0%	12	60.0%	0.206	10	50.0%	10	50.0%	1.000	11	55.0%	9	45.0%	0.527
	>4	9	45.0%	11	55.0%		12	60.0%	8	40.0%		10	50.0%	10	50.0%		9	45.0%	11	55.0%	
Tumor focality	Focal	14	56.0%	11	44.0%	0.327	11	44.0%	14	56.0%	0.327	13	52.0%	12	48.0%	0.744	12	48.0%	13	52.0%	0.744
	Unifocal	6	40.0%	9	60.0%		9	60.0%	6	40.0%		7	46.7%	8	53.3%		8	53.3%	7	46.7%	
Background disease	None	11	52.4%	10	47.6%	0.133	10	47.6%	11	52.4%	0.727	10	47.6%	11	52.4%	0.550	9	42.9%	12	57.1%	0.657
	High blood pressure	6	50.0%	6	50.0%		7	58.3%	5	41.7%		8	66.7%	4	33.3%		7	58.3%	5	41.7%	
	Diabetes	3	100.0%	0	0.0%		2	66.7%	1	33.3%		1	33.3%	2	66.7%		2	66.7%	1	33.3%	
	High blood pressure and diabetes	0	0.0%	3	100.0%		1	33.3%	2	66.7%		1	33.3%	2	66.7%		2	66.7%	1	33.3%	
	Prostate problems	0	0.0%	1	100.0%		0	0.0%	1	100.0%		0	0.0%	1	100.0%		0	0.0%	1	100.0%	
Fuhrman nuclear grade	1	1	20.0%	4	80.0%	0.540	2	40.0%	3	60.0%	0.906	2	40.0%	3	60.0%	0.384	3	60.0%	2	40.0%	0.906
	2	11	52.4%	10	47.6%		11	52.4%	10	47.6%		11	52.4%	10	47.6%		11	52.4%	10	47.6%	
	3	5	55.6%	4	44.4%		4	44.4%	5	55.6%		3	33.3%	6	66.7%		4	44.4%	5	55.6%	
	4	3	60.0%	2	40.0%		3	60.0%	2	40.0%		4	80.0%	1	20.0%		2	40.0%	3	60.0%	
Lymph vascular perineural invasion	No	6	75.0%	2	25.0%	0.114	6	75.0%	2	25.0%	0.114	6	75.0%	2	25.0%	0.114	5	62.5%	3	37.5%	0.429
	Yes	14	43.8%	18	56.3%		14	43.8%	18	56.3%		14	43.8%	18	56.3%		15	46.9%	17	53.1%	
Kidney disease	No	13	44.8%	16	55.2%	0.288	12	41.4%	17	58.6%	0.077	13	44.8%	16	55.2%	0.288	12	41.4%	17	58.6%	0.077
	Yes	7	63.6%	4	36.4%		8	72.7%	3	27.3%		7	63.6%	4	36.4%		8	72.7%	3	27.3%	
Kidney stone	No	12	57.1%	9	42.9%	0.342	12	57.1%	9	42.9%	0.342	8	38.1%	13	61.9%	0.113	12	57.1%	9	42.9%	0.342
	Yes	8	42.1%	11	57.9%		8	42.1%	11	57.9%		12	63.2%	7	36.8%		8	42.1%	11	57.9%	
BMI	≤25	4	44.4%	5	55.6%	0.793	2	22.2%	7	77.8%	0.166	5	55.6%	4	44.4%	0.356	4	44.4%	5	55.6%	0.856
	25–29	14	53.8%	12	46.2%		15	57.7%	11	42.3%		14	53.8%	12	46.2%		13	50.0%	13	50.0%	
	≥30	2	40.0%	3	60.0%		3	60.0%	2	40.0%		1	20.0%	4	80.0%		3	60.0%	2	40.0%	

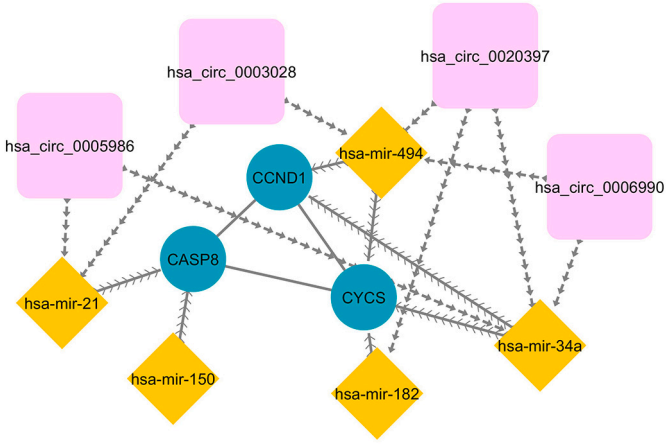

Fig. 4. The ceRNA network of circRNA–DEmiRNA–hub gene in RCC. Rectangles indicate circRNAs, diamonds indicate DEmiRNA, and ellipses indicate hub genes. The solid lines show predicted interactions between protein and protein by the STRING database. The contiguous and separate arrows show predicted DEmiRNA-hub gene and circRNA-DEmiRNA interactions, respectively.

value = 0.038, Fig. 3e). Other circRNAs demonstrated no significant association with RCC subtype and expression (Fig. 3f, g, h). The comparison of expression in different types of RCC was measured two by two. The following are significant *P*-values: The P-value for chromophore and oncocytoma is 0.046; the P-value for clear cell and chromophore is 0.025; and the *P*-value for clear cell and chromophore is 0.032 (Supplementary Files 3).

Furthermore, RCC patients were divided into two groups of high and low expression, according to the median for each gene (Table 8). We did not observe any significant association between low and high expression groups and clinicopathological and demographic features. The significant difference in expression levels found between the RCC and adjacent tissue samples, as well as these relationships, are not proof of the existence of a relationship with clinicopathological characteristics. On the other hand, some clinicopathological factors have no known effect on expression.

3.2. Bioinformatics results

3.2.1. Identification of DEmRNAs

Eighteen gene expression profiles (Table 1, Supplementary Files 2) were collected for analysis. We considered the adjusted *P*-value <0.05 to be statistically significant for DEmRNAs. Totally, 1162 DEmRNAs were screened from 18 GSEs (Supplementary Files 4).

3.2.2. Identification of DEmiRNAs

As shown in Table 3, three miRNA gene chips (GSE16441, GSE55138, and GSE41282) were selected for this study. In the first step, DEmiRNAs were identified by using GEO2R. The threshold points were Adjusted *P*-value <0.05 (Supplementary File 8). Then, we determined common DEmiRNAs in these GSEs.

3.2.3. PPI network construction and identification of hub genes

Common shared DEmRNAs in GSEs were selected for input to the STRING database, and their interaction was constructed (Supplementary Files 4). After the removal of duplicated edges and self-loops, 1130 nodes were displayed in the final network (Supplementary Files 5). After selecting the hubs, in the next steps, we used them to choose the important involved molecular pathways.

3.2.4. Prediction of DEmiRNA-DEmRNA, circRNA-DEmiRNA interactions, and construction of ceRNA network

The list of 50 miRNAs related to DEmRNAs, as well as miRNAs related to the hub genes in the "Pathways in cancer", was detected by miRTarbase, miRDB, PITA, and Targetscan databases using ToppGene (Supplementary File 7). Finally, we chose 12 DEmiRNAs that target hub genes of the "pathways in cancer" (hsa-miR-20a-5p, hsa-miR-182, hsa-miR-20b-5p, hsa-miR-93-5p, hsa-miR-17-5P, hsa-miR-34a, hsa-miR-106b-5p, hsa-miR-206, hsa-miR-150, hsa-miR-122, hsa-miR-21, and hsa-miR-494). CircRNAs play crucial roles in tumors by sponging the miRNAs. We found that three hub genes (*CASP8*; Caspase 8, *CCND1*; Cyclin D1, *CYCS*; Cytochrome C) and five DEmiRNAs (hsa-miR-150, hsa-miR-34a, hsa-miR-494, hsa-miR-182, hsa-miR-21) were regulated by the four circRNAs (hsa_circ_0020397, hsa_circ_0005986, hsa_circ_0003028, hsa_circ_0006990) and based on circRNA-DEmiRNA and DEmiRNA-hub gene interactions we constructed the selected circRNA-associated ceRNA network (Fig. 4).

3.2.5. KEGG pathway enrichment analysis

KEGG pathway enrichment analysis showed involvement of all DEGs in the different pathways such as "Pathways in cancer", "Focal adhesion", "PI3K-Akt signaling pathway", and "mTOR signaling pathway". "Pathways in cancer" was the most significant pathway (Supplementary File 7). It's important to note that this analysis might be overestimate enriched pathways. We highlighted the DEmRNAs in this pathway for subsequent analysis (Supplementary File 7).

3.2.6. Survival analysis

We investigated the overall survival (OS) for three hub genes (*CASP8*, *CCND1*, *CYCS*) in the ceRNA network. Two mRNAs (*CCND1* and *CYCS*) were significantly associated with survival prognosis in RCC patients. CcRCC patients with lower expressions of *CCND1* and *CYCS* had a significantly shorter overall survival (log-rank $p = 2.5e-0.05$ and 0.025), while we did not find a significant association between *CASP8* expressions and survival prognosis in RCC patients (0.17) (Fig. 5). We investigated further by looking at survival analyses in RCC subtypes using the GEPIA database. The log rank p of the results are as follows: 0.023, 0.17, and 0.47 for kidney chromophobe (KICH), kidney renal clear cell carcinoma (KIRC), and kidney renal papillary cell carcinoma (KIRP), respectively (Fig. 6). It should be noted that the results of pan-cancer data for renal cancer have been reported to be significant for the CASP8 (Liu et al., 2021). The available pan-cancer data did not show any differences between RCC subtypes.

4. Discussion

CircRNAs are stable loops, resistant to exonuclease digestion, tissue specificity, and highly abundant. These RNAs have been shown to play key roles as regulators of gene splicing and miRNAs sponges. An increasing number of studies have been carried out to identify the roles circRNAs in malignancies (Tang et al., 2021). Several researches have studied the role of ncRNAs on clinical phenotypes of RCC through their multifaceted biological roles (Franz et al., 2019). In this study, we evaluated hsa_circ_0020397, hsa_circ_0005986, hsa_circ_0003028, and hsa_circ_0006990 expression in RCC compared to their normal tissues. In addition, we used a bioinformatics approach to data mine the various datasets of samples from patients with ccRCC and matched control. To identify DEmRNAs and DEmiRNAs and create a circRNA-associated ceRNA network was our goal. The results are discussed below.

Lower levels of hsa_circ_0020397, hsa_circ_0005986, and hsa_circ_0006990 were detected in patients with RCC, as well as ccRCC subtype, in comparison with the controls using qPCR. Additionally, hsa_circ_0006990 showed a higher expression in oncocytoma type in comparison to other types of RCC. In triple-negative mesenchymal cell lines, hsa_circ_0020397 showed low or undetectable levels, but in epithelial cell lines, regardless of estrogen receptor or HER2 status, its concentration is high (Kurosaki et al., 2021). Zhang et al. reported that via sponging miR-138, hsa_circ_0020397 promoted CRC cell proliferation and invasion, leading to the up-regulation of miR-138 target genes,

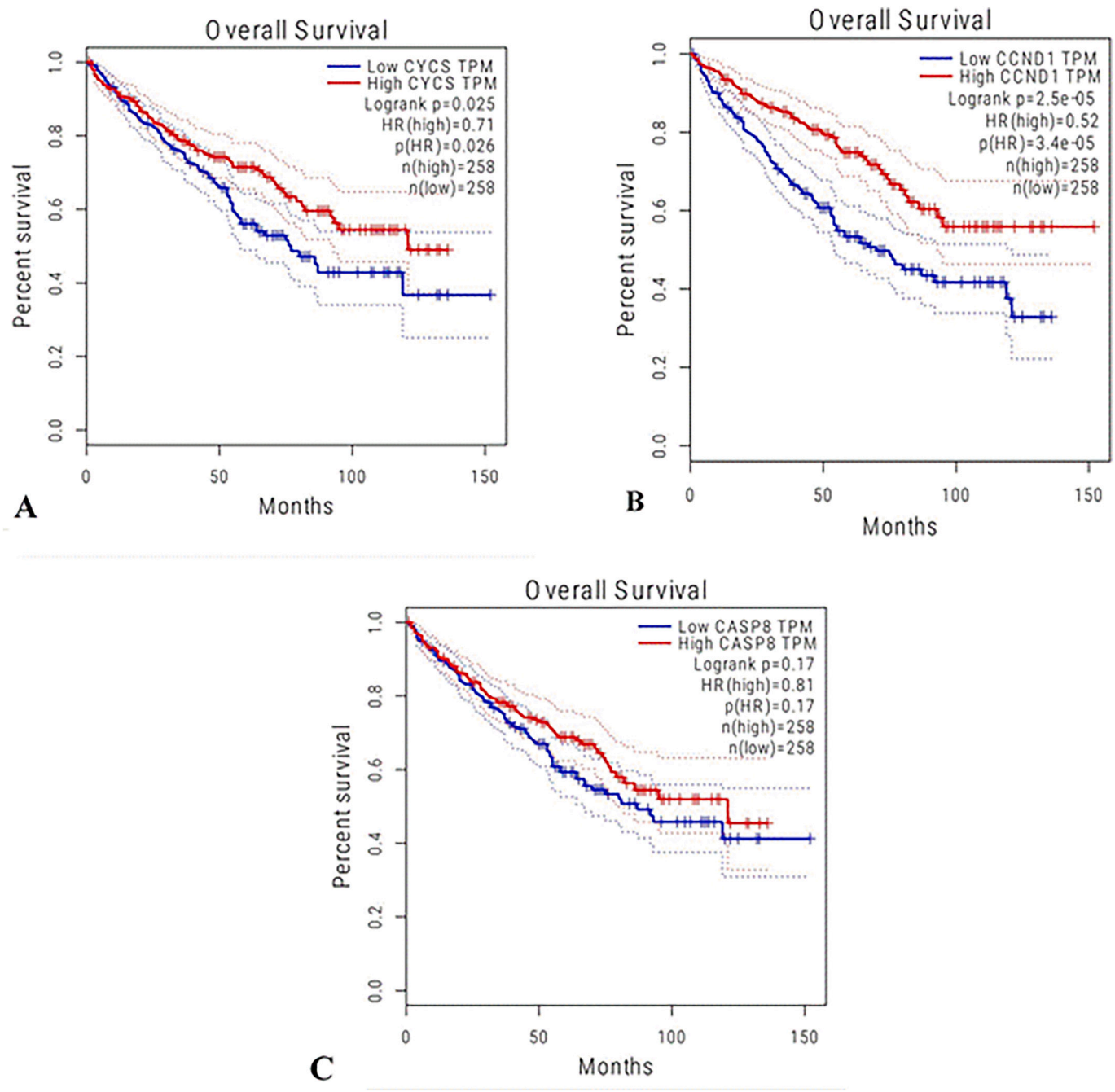

Fig. 5. Overall survival of kidney renal clear cell carcinoma (KIRC) patients based on *CCND1*, *CYCS*, and *CASP8* expression. In relation to *CYCS* and *CCND1*, low expression of the genes was associated with low survival. (A) Log-rank p related to *CYCS* was 0.025. (B) Log-rank p related to *CCND1* was 2.5e-0.5. (C) Log-rank p related to *CASP8* was 0.17.

programmed death-ligand 1 (*PD-L1*), and telomerase reverse transcriptase (*TERT*) (Zhang et al., 2017). These data support our hypothesis that hsa_circ_0020397 contributes to the pathogenesis of RCC. In line with our results, Fu et al. showed that hsa_circ_0005986 is downregulated in HCC. They also showed that this circRNA regulated *NOTCH1* expression by sponging miR-129-5p in a ceRNA manner (Fu et al., 2017). Previous studies reported that hsa_circ_0006990 is a potential CRC biomarker and exerts oncogenic properties via sponging miR-101 (Li et al., 2019). These findings support the idea that hsa_circ_0006990 contributes to the pathophysiology of cancers by acting on the ceRNA regulatory axis. In addition, it was shown that hsa_circ_0003028 is downregulated in urothelial carcinoma and inhibits lymph node invasion in bladder cancer through sponging the miR-570-3p (He et al., 2020). We also found that three types of circRNAs (i.e., hsa_circ_0020397, hsa_circ_0005986, and hsa_circ_0006990) with lower expressions in ccRCC were also downregulated in patients with chronic kidney disease (CKD), which is a known risk factor for RCC (Khan and Pandey, 2014; Pillebout et al., 2003; Rysz et al., 2017). Hence, our findings suggest that the increased risk of RCC in CKD might be related to the downregulation of these 3 cicrRNAs.

Even though there were no significant differences in the hsa_circ_0003028 expression levels between RCC patients and controls in the samples, we discovered that dysregulation of hsa_circ_0003028 is associated with lymphovascular/perineural invasion in RCC patients. In their study on the effects of lymphovascular invasion on survival, Belsante et al. (Belsante et al., 2014) found that patients with lymphovascular invasion had significantly lower rates of disease-free and cancer-

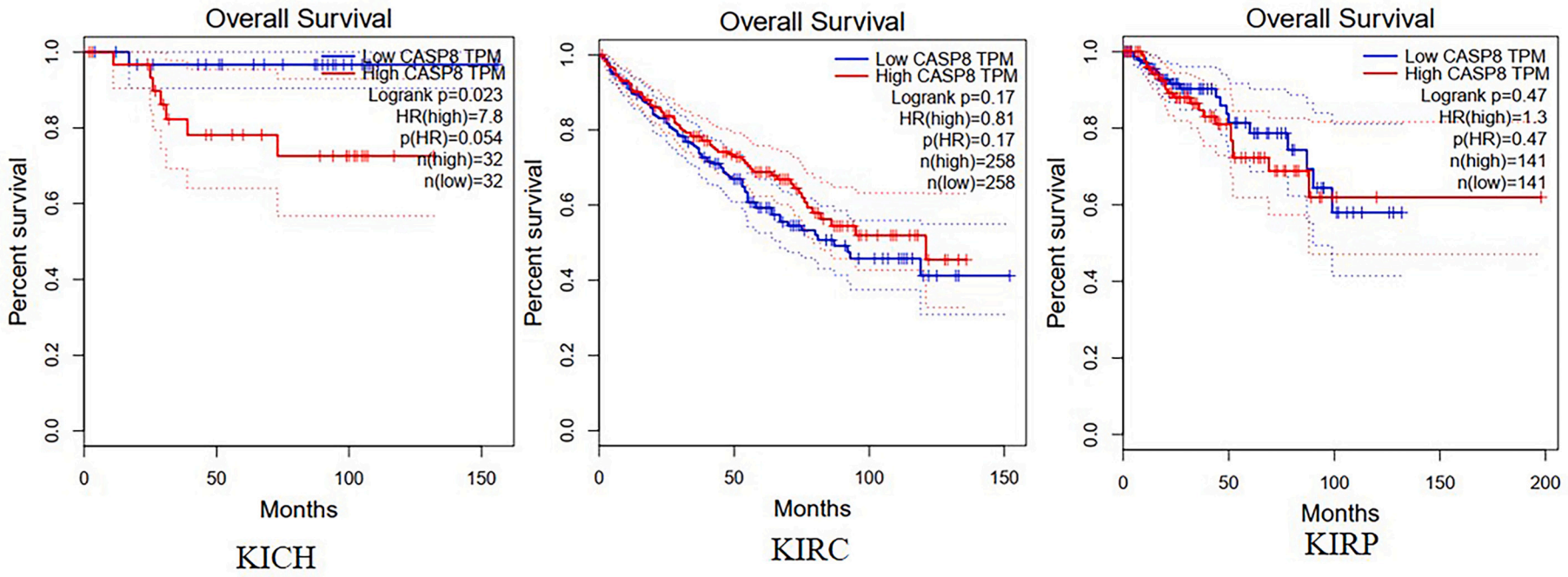

Fig. 6. Overall survival of CASP8 in Kidney chromophobe (KICH), kidney renal clear cell carcinoma (KIRC), and Kidney renal papillary cell carcinoma (KIRP) patients.

specific survival, and they found that lymphovascular invasion was present in 14% of 419 patients with ccRCC. Katz et al. (Katz et al., 2011) found lymphovascular invasion in 11% of 841 patients and found that these patients had considerably poorer rates of metastasis-free, disease-specific, and overall survival. Likewise, perineural invasion of RCCs, is a sign of tumor invasion and metastasis; hence it portends the poor prognosis of patients (Chen et al., 2019). We know that other subtypes of RCC are rare and that ccRCC is the most prevalent form of this malignancy (Hsieh et al., 2017). This might be because the research only has a small sample of each RCC subtype (Supplementary File 1). Given its relatively higher expression in RCCs with lymphovascular/perineural invasion, possible role of hsa_circ_0003028 in lymphovascular/perineural invasion should be further investigated.

According to our bioinformatic results, we predicted the 15 circRNA-DEmiRNA-hub genes ceRNA regulatory axes, which included three hub genes (*CASP8*, *CCND1*, *CYCS*), five DEmiRNAs (hsa-miR-150, hsa-miR-34a, hsa-miR-494, hsa-miR-182, hsa-miR-21), and four circRNAs (hsa_circ_0020397, hsa_circ_0005986, hsa_circ_0003028, hsa_circ_0006990). In recent years, an increasing number of studies have demonstrated that circRNA is crucial to the biological functions of a network of ceRNA (Zhong et al., 2018b). CircRNAs can compete with miRNAs to regulate gene expression at the transcriptional level by affecting the stability of target RNAs or their translation (Zhong et al., 2018b). CircRNAs participate in the biological processes as ceRNAs, including tumor cell proliferation, apoptosis, invasion, and migration (Zhong et al., 2018b). Based on our bioinformatic analysis, we hypothesized that downregulation of hsa_circ_0020397 might increase RCC metastasis through sponging hsa-miR-150 by downregulating *CASP8*. As mentioned above, hsa_circ_0020397 could operate as a tumor suppressor gene in CRC (Zhang et al., 2017). Hsa_circ_0020397 could act to antagonize the activity of miR-138 by affecting its target genes *TERT* and *PDL1*, leading to the invasion and increased cell proliferation in CRC (Zhang et al., 2017). In line with our analysis, one study showed that hsa-miR-150 expression was higher in RCC tissues compared to the normal kidney (Lokeshwar et al., 2018). One of the important genes for regulating apoptosis is *CASP8*, whose activation leads to the activation of caspase-3 (Samaras et al., 2009). The study conducted by Heikaus et al. showed that *CASP8* expression increased during carcinogenesis and downregulated in advanced RCC (Heikaus et al., 2008). In addition, we proposed that hsa_circ_0020397 might sponge hsa-miR-34a and hsa-miR-494. These miRNAs were previously identified to be upregulated (hsa-miR-34a) and downregulated (hsa-miR-494) in RCC tissues compared with the control group (Gattolliat et al., 2018; Toraih et al., 2017). The ceRNA network in our study revealed that hsa-miR-34a and hsa-miR-494 had a link with *CCND1* in the RCC progression. *CCND1*, as an oncogene in many cancers, shows increased expression during the cell cycle. In 2019, it was shown that its expression was upregulated in ccRCC (Wang et al., 2019). In this regard, transcriptomic studies revealed that *CCND1* was overexpressed in RCC cases (Karim et al., 2016). We also demonstrated that hsa_circ_0020397 might down-regulate the *CYCS* expression by sponging hsa-miR-34a. Moreover, the ceRNA network showed that hsa_circ_0020397 sponged hsa-miR-494 and hsa-miR-182. The previous study showed that expression of hsa-miR-494 and hsa-miR-182 were significantly reduced in RCC (Gattolliat et al., 2018; Kulkarni et al., 2018). CYCS is a multifunctional enzyme that plays a role in cell apoptosis and is a mitochondrial biomarker. On the other hand, CYCS has been recently identified as a tumor suppressor in RCC (Liu et al., 2019). Interestingly, our bioinformatics analysis demonstrated that the hsa_circ_0005986 could potentially act as a sponge for some miRNAs (hsa-mir-21, hsa-mir-34a) through given ceRNA networks for regulating its target mRNAs including *CASP8*, *CCND1*, and *CYCS*. In the same vein, we proposed the hsa_circ_0006990 could affect the development of RCC via sponging hsa-mir-494, hsa-mir-34a through *CCND1* and *CYCS*. One of the most significant findings in this research can be a potential function of hsa_circ_0020397/hsa-mir-34a/*CYCS* and hsa_circ_0005986/hsa-mir-34a/*CYCS* axes in the progression of RCC. Although the deregulation of these genes in RCC supports our findings, the anticipated ceRNA axes still require molecular validation. In addition, it is noteworthy that gene expression patterns may be affected by different techniques, patient characteristics, sample preparation, data processing, and platform types.

5. Conclusion

According to our findings, the expression of hsa_circ_0020397, hsa_circ_0005986, and hsa _circ_0006990 was downregulated in RCC tissues. In addition, the expression of these circRNAs was dramatically reduced in patients with a history of kidney illness. In addition, hsa_circ_0003028 and hsa_circ_0006990 demonstrated increased expression in the tumors of participants with lymphovascular/perineural invasion and oncocytoma, respectively. This is the first study to demonstrate the expression of the hsa_circ_0020397, hsa_circ_0005986, hsa_circ_0003028, and hsa_circ_0006990 genes in RCC patients. The reported results are preliminary, and additional in vitro and in vivo studies could potentially strengthen them. This study sheds new light on the molecular pathways behind the formation of RCC, although the potential roles of these circRNAs as ceRNA deserve more investigation.

Supplementary data to this article can be found online at https://doi.org/10.1016/j.yexmp.2022.104848.

Data availability statements

The authors confirm that the data supporting the findings of this study are available within the article and its supplementary materials.

Ethical approval

We have followed all ethical approvals for this study. Ethical approval of this study was granted by the Fasa University of Medical Sciences research ethics committee (ethical code: IR.FUMS.REC.1398.147).

Informed consent

All the participants have signed a consent form.

Funding

This work was supported by Fasa University of Medical Science [grant numbers 97423].

CRediT authorship contribution statement

Elham Mohammadisoleimani: Conceptualization, Investigation, Methodology, Writing – original draft. **Zahra Firoozi:** Formal analysis, Investigation, Methodology, Writing – original draft. **Mohammad Mehdi Naghizadeh:** Conceptualization, Formal analysis. **Ali Ghanbari Asad:** Resources, Writing – review & editing. **Mohammad Hosein Pourjafarian:** Writing – review & editing. **Ali Ariafar:** Methodology, Resources. **Hosein Mansoori:** Resources. **Hassan Dastsooz:** Formal analysis, Validation, Writing – review & editing. **Hani Sabaie:** Investigation, Writing – review & editing. **Shahryar Zeighami:** Methodology, Resources, Supervision. **Yaser Mansoori:** Conceptualization, Investigation, Project administration, Supervision, Writing – original draft.

Declaration of Competing Interest

The authors declare no potential conflicts of interest.

Data availability

Data will be made available on request.

Acknowledgment

The authors are thankful to patients who took part in this study.

References

Abdollahzadeh, R., Daraei, A., Mansoori, Y., Sepahvand, M., Amoli, M.M., Tavakkoly-Bazzaz, J., 2019. Competing endogenous RNA (ceRNA) cross talk and language in ceRNA regulatory networks: a new look at hallmarks of breast cancer. J. Cell. Physiol. 234 (7), 10080–10100.

Ala, U., 2020. Competing endogenous RNAs, non-coding RNAs and diseases: an intertwined story. Cells. 9 (7).

Ankasha, S.J., Shafiee, M.N., Wahab, N.A., Ali, R.A.R., Mokhtar, N.M., 2018. Post-transcriptional regulation of microRNAs in cancer: from prediction to validation. Oncol. Rev. 12 (1), 344.

Arai, E., Kanai, Y., 2010. Genetic and epigenetic alterations during renal carcinogenesis. Int. J. Clin. Exp. Pathol. 4 (1), 58–73.

Bai, S., Wu, Y., Yan, Y., Shao, S., Zhang, J., Liu, J., et al., 2020. Construct a circRNA/miRNA/mRNA regulatory network to explore potential pathogenesis and therapy options of clear cell renal cell carcinoma. Sci. Rep. 10 (1), 13659.

Belsante, M., Darwish, O., Youssef, R., Bagrodia, A., Kapur, P., Sagalowsky, A.I., et al., 2014. Lymphovascular invasion in clear cell renal cell carcinoma–association with disease-free and cancer-specific survival. Urol. Oncol. 32 (1), 30.e23–8.

Chen, S.H., Zhang, B.Y., Zhou, B., Zhu, C.Z., Sun, L.Q., Feng, Y.J., 2019. Perineural invasion of cancer: a complex crosstalk between cells and molecules in the perineural niche. Am. J. Cancer Res. 9 (1), 1–21.

Chen, Y.Y., Hu, H.H., Wang, Y.N., Liu, J.R., Liu, H.J., Liu, J.L., et al., 2020. Metabolomics in renal cell carcinoma: from biomarker identification to pathomechanism insights. Arch. Biochem. Biophys. 695, 108623.

De Meerleer, G., Khoo, V., Escudier, B., Joniau, S., Bossi, A., Ost, P., et al., 2014. Radiotherapy for renal-cell carcinoma. Lancet Oncol. 15 (4), e170–e177.

Edgar, R., Domrachev, M., Lash, A.E., 2002. Gene expression omnibus: NCBI gene expression and hybridization array data repository. Nucleic Acids Res. 30 (1), 207–210.

Franz, A., Ralla, B., Weickmann, S., Jung, M., Rochow, H., Stephan, C., et al., 2019. Circular RNAs in clear cell renal cell carcinoma: their microarray-based identification, analytical validation, and potential use in a Clinico-genomic model to improve prognostic accuracy. Cancers (Basel). 11 (10).

Fu, L., Chen, Q., Yao, T., Li, T., Ying, S., Hu, Y., et al., 2017. Hsa_circ_0005986 inhibits carcinogenesis by acting as a miR-129-5p sponge and is used as a novel biomarker for hepatocellular carcinoma. Oncotarget. 8 (27), 43878–43888.

Gattolliat, C.H., Couvé, S., Meurice, G., Oréar, C., Droin, N., Chiquet, M., et al., 2018. Integrative analysis of dysregulated microRNAs and mRNAs in multiple recurrent synchronized renal tumors from patients with von Hippel-Lindau disease. Int. J. Oncol. 53 (4), 1455–1468.

Glažar, P., Papavasileiou, P., Rajewsky, N., 2014. circBase: a database for circular RNAs. Rna. 20 (11), 1666–1670.

He, Q., Yan, D., Dong, W., Bi, J., Huang, L., Yang, M., et al., 2020. circRNA circFUT8 upregulates Krüpple-like factor 10 to inhibit the metastasis of bladder Cancer via sponging miR-570-3p. Mol. Ther. Oncolytics. 16, 172–187.

Heikaus, S., Kempf, T., Mahotka, C., Gabbert, H.E., Ramp, U., 2008. Caspase-8 and its inhibitors in RCCs in vivo: the prominent role of ARC. Apoptosis. 13 (7), 938–949.

Hsieh, J.J., Purdue, M.P., Signoretti, S., Swanton, C., Albiges, L., Schmidinger, M., et al., 2017. Renal cell carcinoma. Nat. Rev. Dis. Primers. 3, 17009.

Jiang, W.-d., Ye, Z.-h., 2019. Integrated analysis of a competing endogenous RNA network in renal cell carcinoma using bioinformatics tools. Biosci. Rep. 39 (7).

Karim, S., Al-Maghrabi, J.A., Farsi, H.M., Al-Sayyad, A.J., Schulten, H.J., Buhmeida, A., et al., 2016. Cyclin D1 as a therapeutic target of renal cell carcinoma- a combined transcriptomics, tissue microarray and molecular docking study from the Kingdom of Saudi Arabia. BMC Cancer 16 (Suppl. 2), 741.

Katz, M.D., Serrano, M.F., Humphrey, P.A., Grubb 3rd, R.L., Skolarus, T.A., Gao, F., et al., 2011. The role of lymphovascular space invasion in renal cell carcinoma as a prognostic marker of survival after curative resection. Urol. Oncol. 29 (6), 738–744.

Khan, Z., Pandey, M., 2014. Role of kidney biomarkers of chronic kidney disease: an update. Saudi. J. Biol. Sci. 21 (4), 294–299.

Kulkarni, P., Dasgupta, P., Bhat, N.S., Shahryari, V., Shiina, M., Hashimoto, Y., et al., 2018. Elevated miR-182-5p associates with renal Cancer cell mitotic arrest through diminished MALAT-1 expression. Mol. Cancer Res. 16 (11), 1750–1760.

Kurosaki, M., Terao, M., Liu, D., Zanetti, A., Guarrera, L., Bolis, M., et al., 2021. A DOCK1 gene-derived circular RNA is highly expressed in luminal mammary Tumours and is involved in the epithelial differentiation, growth, and motility of breast Cancer cells. Cancers (Basel). 13 (21).

Li, Z., Huang, C., Bao, C., Chen, L., Lin, M., Wang, X., et al., 2015. Exon-intron circular RNAs regulate transcription in the nucleus. Nat. Struct. Mol. Biol. 22 (3), 256–264.

Li, B., Wang, F., Li, X., Sun, S., Shen, Y., Yang, H., 2018. Hsa_circ_0008309 may be a potential biomarker for Oral squamous cell carcinoma. Dis. Markers 2018, 7496890.

Li, X.N., Wang, Z.J., Ye, C.X., Zhao, B.C., Huang, X.X., Yang, L., 2019. Circular RNA circVAPA is up-regulated and exerts oncogenic properties by sponging miR-101 in colorectal cancer. Biomed. Pharmacother. 112, 108611.

Li, L., Sun, D., Li, X., Yang, B., Zhang, W., 2021. Identification of key circRNAs in non-small cell lung Cancer. Am J Med Sci 361 (1), 98–105.

Liu, Z., Zhao, X., Zhang, L., Pei, B., 2019. Cytochrome C inhibits tumor growth and predicts favorable prognosis in clear cell renal cell carcinoma. Oncol. Lett. 18 (6), 6026–6032.

Liu, S., Garcia-Marques, F., Zhang, C.A., Lee, J.J., Nolley, R., Shen, M., et al., 2021. Discovery of CASP8 as a potential biomarker for high-risk prostate cancer through a high-multiplex immunoassay. Sci. Rep. 11 (1), 7612.

Lokeshwar, S.D., Talukder, A., Yates, T.J., Hennig, M.J.P., Garcia-Roig, M., Lahorewala, S.S., et al., 2018. Molecular characterization of renal cell carcinoma: a potential three-MicroRNA prognostic signature. Cancer Epidemiol. Biomark. Prev. 27 (4), 464–472.

Mendoza-Alvarez, A., Guillen-Guio, B., Baez-Ortega, A., Hernandez-Perez, C., Lakhwani-Lakhwani, S., M-d-C, Maeso, et al., 2019. Whole-exome sequencing identifies somatic mutations associated with mortality in metastatic clear cell kidney carcinoma. Front. Genet. 10.

Moch, H., Srigley, J., Delahunt, B., Montironi, R., Egevad, L., Tan, P.H., 2014. Biomarkers in renal cancer. Virchows Arch. 464 (3), 359–365.

Muglia, V.F., Prando, A., 2015. Renal cell carcinoma: histological classification and correlation with imaging findings. Radiol. Bras. 48 (3), 166–174.

O'Brien, J., Hayder, H., Zayed, Y., Peng, C., 2018. Overview of MicroRNA biogenesis, mechanisms of actions, and circulation. Front Endocrinol. (Lausanne) 9, 402.

Panda, A.C., Gorospe, M., 2018. Detection and analysis of circular RNAs by RT-PCR. Bio. Protoc. 8 (6).

Pillebout, E., Weitzman, J.B., Burtin, M., Martino, C., Federici, P., Yaniv, M., et al., 2003. JunD protects against chronic kidney disease by regulating paracrine mitogens. J. Clin. Invest. 112 (6), 843–852.

Rysz, J., Gluba-Brzózka, A., Franczyk, B., Jabłonowski, Z., Ciałkowska-Rysz, A., 2017. Novel biomarkers in the diagnosis of chronic kidney disease and the prediction of its outcome. Int. J. Mol. Sci. 18 (8).

Salmena, L., Poliseno, L., Tay, Y., Kats, L., Pandolfi, P.P., 2011. A ceRNA hypothesis: the Rosetta stone of a hidden RNA language? Cell. 146 (3), 353–358.

Samaras, V., Tsopanomichalou, M., Stamatelli, A., Arnaoutoglou, C., Samaras, E., Arnaoutoglou, M., et al., 2009. Is there any potential link among caspase-8, p-p38 MAPK and bcl-2 in clear cell renal cell carcinomas? A comparative immunohistochemical analysis with clinical connotations. Diagn. Pathol. 4, 7.

Santer, L., Bär, C., Thum, T., 2019. Circular RNAs: a novel class of functional RNA molecules with a therapeutic perspective. Mol. Ther. 27 (8), 1350–1363.

Sayad, A., Najafi, S., Kashi, A.H., Hosseini, S.J., Akrami, S.M., Taheri, M., et al., 2022. Circular RNAs in renal cell carcinoma: functions in tumorigenesis and diagnostic and prognostic potentials. Pathol. Res. Pract. 229, 153720.

Shannon, P., Markiel, A., Ozier, O., Baliga, N.S., Wang, J.T., Ramage, D., et al., 2003. Cytoscape: a software environment for integrated models of biomolecular interaction networks. Genome Res. 13 (11), 2498–2504.

Shin Lee, J., Seok Kim, H., Bok Kim, Y., Cheol Lee, M., Soo, Park C., 2003. Expression of PTEN in renal cell carcinoma and its relation to tumor behavior and growth. J. Surg. Oncol. 84 (3), 166–172.

Si, W., Shen, J., Zheng, H., Fan, W., 2019. The role and mechanisms of action of microRNAs in cancer drug resistance. Clin. Epigenetics 11 (1), 25.

Szklarczyk, D., Gable, A.L., Lyon, D., Junge, A., Wyder, S., Huerta-Cepas, J., et al., 2019. STRING v11: protein-protein association networks with increased coverage, supporting functional discovery in genome-wide experimental datasets. Nucleic Acids Res. 47 (D1), D607–d13.

Tang, Z., Li, C., Kang, B., Gao, G., Li, C., Zhang, Z., 2017. GEPIA: a web server for cancer and normal gene expression profiling and interactive analyses. Nucleic Acids Res. 45 (W1), W98–w102.

Tang, X., Ren, H., Guo, M., Qian, J., Yang, Y., Gu, C., 2021. Review on circular RNAs and new insights into their roles in cancer. Comput. Struct. Biotechnol. J. 19, 910–928.

Toraih, E.A., Ibrahiem, A.T., Fawzy, M.S., Hussein, M.H., Al-Qahtani, S.A.M., Shaalan, A. A.M., 2017. MicroRNA-34a: a key regulator in the hallmarks of renal cell carcinoma. Oxidative Med. Cell. Longev. 2017, 3269379.

Toraih, E.A., Sedhom, J.A., Haidari, M., Fawzy, M.S., 2022. Chapter 7 - applications of noncoding RNAs in renal cancer patients. In: Gupta, S.C., Challagundla, K.B. (Eds.), Clinical Applications of Noncoding RNAs in Cancer. Academic Press, pp. 211–284.

Wang, Q.S., Li, F., Liao, Z.Q., Li, K., Yang, X.L., Lin, Y.Y., et al., 2019. Low level of cyclin-D1 correlates with worse prognosis of clear cell renal cell carcinoma patients. Cancer Med. 8 (9), 4100–4109.

Wang, Y., Zhang, Y., Wang, P., Fu, X., Lin, W., 2020. Circular RNAs in renal cell carcinoma: implications for tumorigenesis, diagnosis, and therapy. Mol. Cancer 19 (1), 149.

Yan, L., Zhang, Y., Ding, B., Zhou, H., Yao, W., Xu, H., 2019. Genetic alteration of histone lysine methyltransferases and their significance in renal cell carcinoma. PeerJ. 7, e6396.

Zhang, X.L., Xu, L.L., Wang, F., 2017. Hsa_circ_0020397 regulates colorectal cancer cell viability, apoptosis and invasion by promoting the expression of the miR-138 targets TERT and PD-L1. Cell Biol. Int. 41 (9), 1056–1064.

Zhang, Z., Xie, Q., He, D., Ling, Y., Li, Y., Li, J., et al., 2018. Circular RNA: new star, new hope in cancer. BMC Cancer 18 (1), 834.

Zhang, W., Zheng, X., Xie, S., Zhang, S., Mao, J., Cai, Y., et al., 2020. TBOPP enhances the anticancer effect of cisplatin by inhibiting DOCK1 in renal cell carcinoma. Mol. Med. Rep. 22 (2), 1187–1194.

Zhong, S., Wang, J., Zhang, Q., Xu, H., Feng, J., 2018a. CircPrimer: a software for annotating circRNAs and determining the specificity of circRNA primers. BMC Bioinform. 19 (1), 292.

Zhong, Y., Du, Y., Yang, X., Mo, Y., Fan, C., Xiong, F., et al., 2018b. Circular RNAs function as ceRNAs to regulate and control human cancer progression. Mol. Cancer 17 (1), 79.